

Whole-Organism Imaging of Spinal Motor Neurons and Musculature with the Agilent BioTek Cytation C10 Confocal Imaging Reader

Author

Rebecca Mongeon, PhD
Agilent Technologies, Inc.

Abstract

Zebrafish present an unparalleled opportunity for *in vivo* neuromuscular disease research. The combination of optical transparency and genetic manipulability provides a uniquely tractable system in which to probe vertebrate spinal motor neuron and muscle function. Light microscopy is an invaluable tool in phenotypic examination of zebrafish, and confocal microscopy is essential to resolve subcellular details when imaging deep within the intact zebrafish embryo. This application note demonstrates how a single automated instrument provides a powerful combination of widefield microscopy and high-resolution confocal microscopy necessary for microscopy investigations in whole organisms, such as zebrafish.

Introduction

Zebrafish have long held an essential role in developmental biology research due to their many and often cited advantages, both biological and practical. Recently, zebrafish amenability to genome editing techniques such as CRISPR, high-throughput screening, and predictive value in drug discovery toxicology studies¹, combined with their exceptional accessibility to optogenetic manipulation and live-imaging techniques highlight the essential place zebrafish have in the toolkit of health-driven research. Indeed, zebrafish are lowering the barrier to *in vivo* research of devastating neurodegenerative diseases, such as amyotrophic lateral sclerosis (ALS, also known as Lou Gehrig's disease)², as their complete spinal neuron and muscle unit organization is entirely accessible to observation through light microscopy.

This application brief demonstrates the capability of whole-organism imaging on the Agilent BioTek Cytation C10 confocal imaging reader, with a focus on spinal motor neurons, neuromuscular synapses, and musculature of the zebrafish model organism. The optical sectioning of the spinning disk confocal system is essential to resolving the deep tissue structures, such as the fine neuronal processes, and provides a literal clearer view of subcellular details when imaging thick samples.

Experimental

Unless otherwise noted, all chemicals were obtained from Sigma Aldrich (St. Louis, MO). General maintenance of zebrafish followed established methods.³ Wild-type male and female *Danio rerio* were maintained at 28 °C on a 14-/10-hour light/dark cycle. Adults were crossed and eggs promptly collected in EM3 media.⁴ To reduce pigmentation, embryos were treated with 0.003% N-phenylthiourea in EM3 starting at 24 hours post-fertilization. Embryos were prepared for immunohistochemistry and staining as follows: at 3 days post-fertilization (pec-fin stage), embryos were manually dechorionated, anesthetized and fixed with 4% paraformaldehyde (PFA) in phosphate-buffered saline (PBS) at 4 °C overnight. Following incubation, fixed embryos were removed from PFA and rinsed with PBS-1% Tween20 (PBST). Embryos were permeabilized in consecutive steps as follows: fixed embryos were rinsed in ddH₂O, submerged in pre-chilled acetone for 8 minutes at -20 °C, rinsed with ddH₂O, followed by a final rinse in PBST. Embryos were then incubated at RT for one hour in permeabilization buffer (PBST with 3% TritonX-100 and 1% DMSO), followed by incubation at RT for one hour in blocking buffer

(PBST with 3% BSA, 1% TritonX-100 and 1% DMSO). Permeabilized and blocked embryos were incubated overnight at 4 °C in a primary antibody and stain mixture of 1:200 DAPI, part number D1306, from Invitrogen (Carlsbad, CA), 1:100 phalloidin-Alexa Fluor 488, part number A12379, from Invitrogen (Carlsbad, CA), 1:200 α -bungarotoxin-Alexa Fluor 555, part number B35451, from Invitrogen (Carlsbad, CA) and 1:100 anti-acetylated tubulin, part number SAB5600134, from Sigma Aldrich (St. Louis, MO) in blocking buffer. Following incubation, embryos were rinsed extensively and incubated at RT in PBST for 3 hours. Embryos were next incubated overnight at 4 °C with secondary antibody - anti-rabbit Alexa Fluor 647, 4414S, from Cell Signaling Technology (Danvers, MA) - followed by extensive rinsing with PBST. Embryos were mounted for imaging in glass-bottom 35 mm dishes, part number P35G-1.5-20-C, from MatTek (Ashland, MA) with 1.5% agarose in PBS.

Imaging procedure and processing

The Cytation C10 confocal imaging reader and Agilent BioTek Gen5 microplate reader and imager software were used to acquire all images, including brightfield, widefield and confocal images. The Cytation C10 instrument was equipped with a 40 μ m pinhole spinning disk, Hamamatsu Orca sCMOS camera, and emission/excitation filter cubes for both confocal and widefield modes as follows (widefield: DAPI 1225100, GFP 1225101, TRITC 1225125, CY5 1225105; confocal: DAPI 1945103, GFP 1945104, TRITC 1945106, CY5 1945102). Low magnification (4x) images are displayed "raw", without further image processing, and contain a single z-height. Higher magnification images (40x) were acquired as a z-stack at 1 μ m intervals, for both widefield and confocal modalities. Z-projections were summated using Gen5 "Maximum" method and subsequently processed in Gen5 to flatten background with a 50 μ m rolling ball diameter in all fluorescence channels, except green (no processing). For 3D rendering, all images in the z-stack were first background flattened (20 μ m rolling ball, all channels), and subsequently opened in the Gen5 3D viewer application. To display only a single zebrafish somite, renderings were cropped using the 3D viewer functionality. Static images of 3D renderings were obtained with the 3D viewer "Snapshot" feature, and videos obtained with the "Record Video" feature."

Results and discussion

Low magnification widefield fluorescence images (4x) provide an excellent staining overview (Figure 1A). DAPI labels nuclei with highest densities observed through the head and spinal cord, and diffuse labeling throughout the skin. Phalloidin labels actin filaments that are particularly enriched throughout skeletal musculature. α -bungarotoxin staining of acetylcholine receptors indicates primarily diffuse staining through musculature at 4x magnification, but higher magnification reveals typical punctate pattern of neuromuscular synapse staining, as seen in Figure 2. Acetyl- α -tubulin staining identifies neuronal axons, visible throughout cranial nerves, spinal cord and lateral line. Expected yolk autofluorescence is also observed in green and orange emission channels.

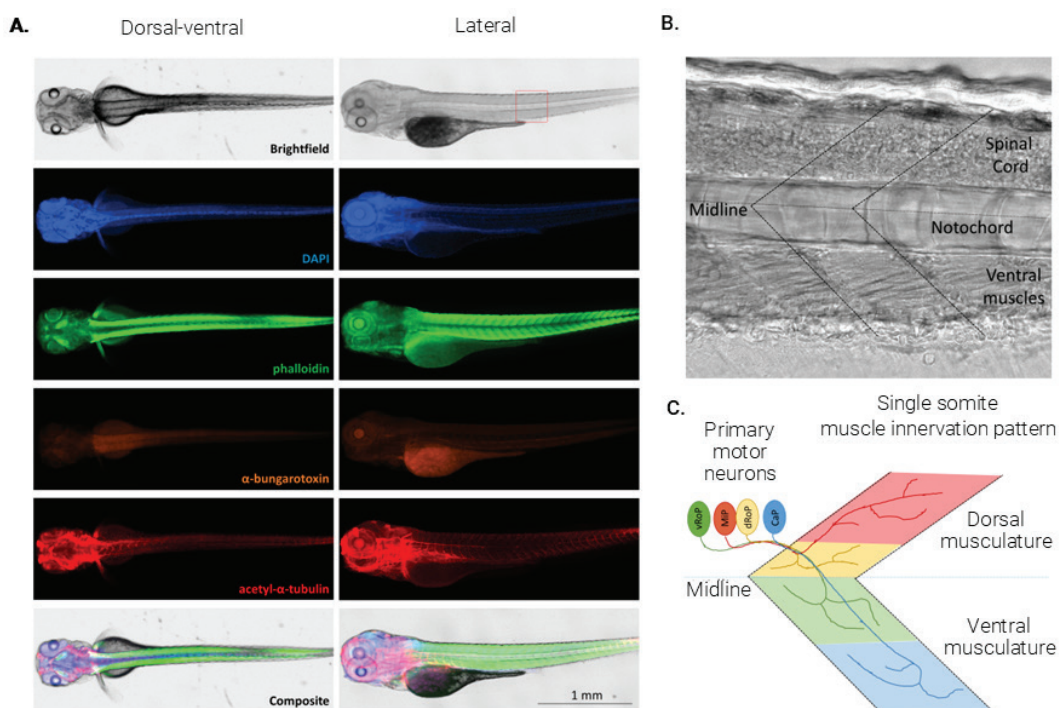


Figure 1. Zebrafish structure and staining overview using automated widefield mode on Agilent BioTek Cytation C10 confocal imaging reader. (A.) Dorsal-ventral and lateral mounting views of 3 days post-fertilization zebrafish embryo taken at 4x magnification. The stains underlying the signal for each color channel are indicated in the left panels. The red square in the lateral brightfield image indicates the region used for higher magnification in (B.). (B.) 40x magnification brightfield image of mid-tail region 50 μ m depth below the skin, approximately at the center of the left-right axis (sagittal plane midline) and spinal cord. Neuron cell bodies are visible as densely-packed round or balloon-shaped cells throughout the spinal cord. The notochord, a cartilage-like precursor to the bony vertebrae, and ventral muscle cells are indicated. Dashed chevron-shaped overlay indicates the outline of a single somite, a repeating body structure that contains a functional unit of primary motor neurons and musculature. (C.) Depiction of the structure of the somite motor units, including primary motor neurons that innervate their respective zones of musculature.

At higher magnification, as shown in Figure 1B, much of the general organization of the spinal cord and musculature can be appreciated using brightfield illumination, including the chevron-shaped repeating units called somites. Each somite contains primary motor neurons and their field of innervated musculature (Figure 1C) with the apparent number of motor neurons depending on developmental stage.^{5,6} The embryonic zebrafish motor unit organization, paired with their size and transparency, allows for unprecedented access to primary motor neuron outgrowth, innervation, and degeneration using confocal microscopy and makes zebrafish models particularly well-suited for neuropathy disease research.

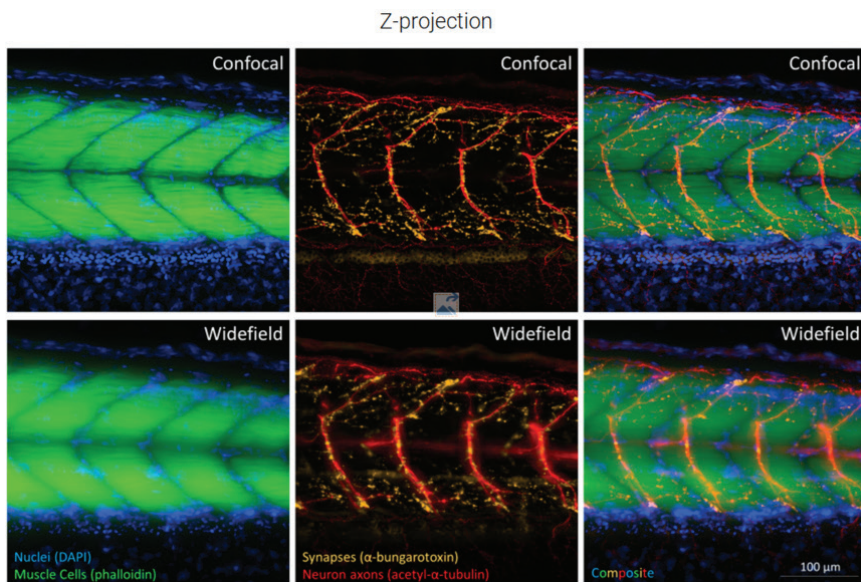


Figure 2. Agilent BioTek Cytation C10 confocal imaging reader confocal mode and widefield mode image comparison of zebrafish axial neuromuscular units. 40x magnification spinning disk (40 μm pinhole) confocal z-projection (top row) and widefield z-projection (bottom row). Staining underlying signal for each color channel is as indicated in the lower panels.

At higher magnification (Figure 2, 40x), z-stacks were acquired every 1 μm from the skin surface to just beyond the sagittal midline plane (~80 μm depth) to capture the entire left side of the embryo. The images displayed in Figure 2 were generated from maximal z-projections in Gen5 software from a subsection of the stack starting at 25 μm depth to 50 μm depth. This subsection of the z-stack best captured motor neuron structures by avoiding the additional neuron axon staining observed close to the skin surface. For this comparison, both confocal and widefield z-projection images were identically processed with a 50 μm rolling ball background reduction step. Although all four color channels were acquired simultaneously, channels are displayed in pairs for clarity. Confocal images show clearly improved contrast and apparent resolution in all channels and all structures, from identification of individual nuclei and muscle cells at depth, to fine neuronal processes and subcellular synaptic junctions that decorate neuronal axons. The observed staining of the axon tracts is consistent with the projection and arborization of the primary motor neurons indicated in Figure 1, and are likely to include CaP, MiP and RoP motoneurons in each somite.

The 3D viewer module of Gen5 is an interactive display of the z-stacks that allows for free rotation and observation of samples around all axes. 3D renderings provide an opportunity to better examine and visualize the spatial relationships between structures imaged over the depth of the z-stack. For clarity, only muscle (green) and neuron (red) channels were included in the rendering snapshots shown in Figure 3. Cropping tools within the 3D Viewer package were used to reduce the full images (as seen in Figure 2) into a single somite to allow for the architecture of just a single somite to be observed in cross-section. In the lateral view, the rendering includes only slices from 20 to 50 μm depth, to allow viewing of motor neurons and reduce views of superficial axons near the skin surface. The cross-section view includes the full depth of images (50 μm). From the confocal rendered cross-section perspective, the structure of the motor unit can be more fully appreciated, with neuron axons curving along the musculature boundary against the spinal cord (SC) and notochord (N) before branching out laterally and innervating the depth of the musculature (arrowhead example). Superficial neuron axon staining of the lateral line (LL) and axons throughout the skin is also observed. The confocal functionality is essential to observing these structures, as out-of-focus light obscures the cross-section obtained in widefield mode for this thick sample (right panel).

In addition to static snapshots pictured in Figure 3, the interactive 3D viewer software module generates videos for offline viewing, wherein samples are rotated around a chosen axis. In the video link below, three somites with neuron (red) and muscle (green) staining are 3D rendered and rotated round the y-axis, corresponding to the sagittal (left-right) midline axis of the embryo.

[Cytation C10 confocal zebrafish motor neuron axons and muscle cells video](#)

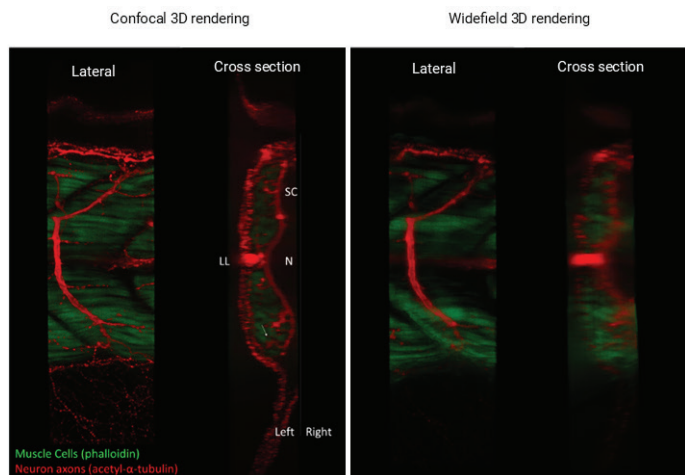


Figure 3. Agilent BioTek Gen5 3D viewer software package for Agilent BioTek Cytation C10 confocal imaging reader renders z-stacks of a single zebrafish somite. Snapshots from the Agilent BioTek Gen5 microplate reader and imager software 3D rendering module of the zebrafish embryo z-stacks from lateral and cross-section perspectives. Stain identities as indicated in confocal (left) panel. Annotations added to the cross-section panel indicate locations of spinal cord (SC), notochord (N), lateral line (LL) and left-right body axis midline (dashed line). Arrowhead indicates an example of a neuron process innervating deeply into the musculature.

Conclusion

The Agilent BioTek Cytation C10 confocal imaging reader excels at imaging of single cells in whole-mount zebrafish samples, demonstrating substantial improvements to image contrast and resolution of fluorescence signals at depth compared to widefield modality. The image improvements derived from the confocal optical sectioning enables detailed 3D rendering of cells deep in tissue, while still maintaining the ease of usability of the Cytation automated imaging system.

References

1. Ali, S.; van Mil, H.G.J.; and Richardson, M.K. (2011) Large-Scale Assessment of the Zebrafish Embryo as a Possible Predictive Model in Toxicity Testing. *PLoS ONE* 6(6): e21076. doi:[10.1371/journal.pone.0021076](https://doi.org/10.1371/journal.pone.0021076)
2. Asakawa, K.; Handa, H.; and Kawakami, K. (2021) Illuminating ALS Motor Neurons with Optogenetics in Zebrafish. *Front. Cell Dev. Biol.* 9:640414. doi:[10.3389/fcell.2021.640414](https://doi.org/10.3389/fcell.2021.640414)
3. Westerfield, M. (2000) *The Zebrafish Book: A Guide for the Laboratory Use of Zebrafish (Danio rerio)*. 4th ed. Eugene: Univ. of Oregon Press. Accessed at https://zfin.org/zf_info/zfbook/zfbk.html
4. Avdesh, A.; Chen, M.; Martin-Iverson, M.T.; Mondal, A.; Ong, G.; Rainey-Smith, S.; Taddei, K.; Lardelli, M.; Groth, D.M.; Verdile, G.; and Martins, R.N. (2012) Regular Care and Maintenance of a Zebrafish (*Danio rerio*) Laboratory: An Introduction. *J. Vis. Exp.* 69:e4196. doi:[10.3791/4196](https://doi.org/10.3791/4196)
5. Bello-Rojas, A.; Istrate, A.E.; Kishore, S.; and McLean, D.L. (2019) Central and Peripheral Innervation Patterns of Definitive Axial Motor Units in Larval Zebrafish. *J. Comp. Neurol.* 527:2557-2572. doi:[10.1002/cne.24689](https://doi.org/10.1002/cne.24689)
6. Issa, F.A.; Mock, A.F.; Sagasti, A.; and Papazian, D.M. (2012) Spinocerebellar Ataxia Type 13 Mutation that is Associated with Disease Onset in Infancy Disrupts Axonal Pathfinding During Neuronal Development. *Dis. Model. Mech.* 5:921-929. doi:[10.1242/dmm.010157](https://doi.org/10.1242/dmm.010157)

www.agilent.com/lifesciences/biotek

For Research Use Only. Not for use in diagnostic procedures.

RA44329.3438194444

This information is subject to change without notice.

© Agilent Technologies, Inc. 2021
Published in the USA, December 1, 2021
5994-4061EN

